

We are IntechOpen, the world's leading publisher of Open Access books Built by scientists, for scientists

6,100

Open access books available

149,000

International authors and editors

185M

Downloads

Our authors are among the

154

Countries delivered to

TOP 1%

most cited scientists

12.2%

Contributors from top 500 universities



WEB OF SCIENCE™

Selection of our books indexed in the Book Citation Index
in Web of Science™ Core Collection (BKCI)

Interested in publishing with us?
Contact book.department@intechopen.com

Numbers displayed above are based on latest data collected.
For more information visit www.intechopen.com



Chapter

Erosion Control at Downstream of Reservoir Using In-stream Weirs

Yaoxin Zhang, Yafei Jia, Keh-Chia Yeh and Chung-Ta Liao

Abstract

As low-head hydraulic structures, instream weirs are built across rivers to control the upstream water surface elevation and the downstream flow conditions. This chapter presents a study of erosion control using instream weirs at downstream of a reservoir; Jiji Weir was built across the longest river in Taiwan, Chuoshui Creek, a mountainous river with steep slopes. Due to the easy-to-be-eroded fine lithology layers of mud, shiver, and sandstones on channel bed, the downstream of Jiji Weir had suffered from severe channel incision and head-cut development problems, which greatly threatens the integrity of the dam. To protect the Jiji Weir and its downstream channel from serious channel erosions, the Water Resources Agency (WRA) of Taiwan proposed erosion control plans that multiple instream weir structures were to be installed along the downstream channel of Jiji Weir. A three-dimensional (3D) numerical model, CCHE3D model with capabilities of simulating bedrock erosions, was used to evaluate those erosion control plans and thus explore for the optimal design.

Keywords: instream-weir, bedrock erosion, channel incision, erosion control, three-dimensional model

1. Introduction

Jiji Weir was built across Chuoshui River, the longest river (178.6 km) in Taiwan, originating from the central mountains and flowing into the East China Sea, covering a watershed about 4323 km². A shallow reservoir was formed due to the construction of the weir. The precipitation and geology dominate the flow and sedimentation processes in the channel and the reservoir. Particularly, during typhoon seasons, floods with high discharges will carry a large amount of sediments flowing through the river channel. Shortly after the weir construction, a pebble-boulder-sized sedimentation layer covering the channel bed was mobilized by the initial clear water releases, and the soft rocks beneath this sedimentation layer were exposed. Within the 6.5 km region downstream of the dam, the channel bed now is featured with erodible lithology layers of mud, shiver, and sandstones, resulted from severe channel incisions and a head-cut development. According to the comparisons of historical longitudinal profiles in **Figure 1**, the vertical incision of the channel thalweg from 2002 to 2014 is

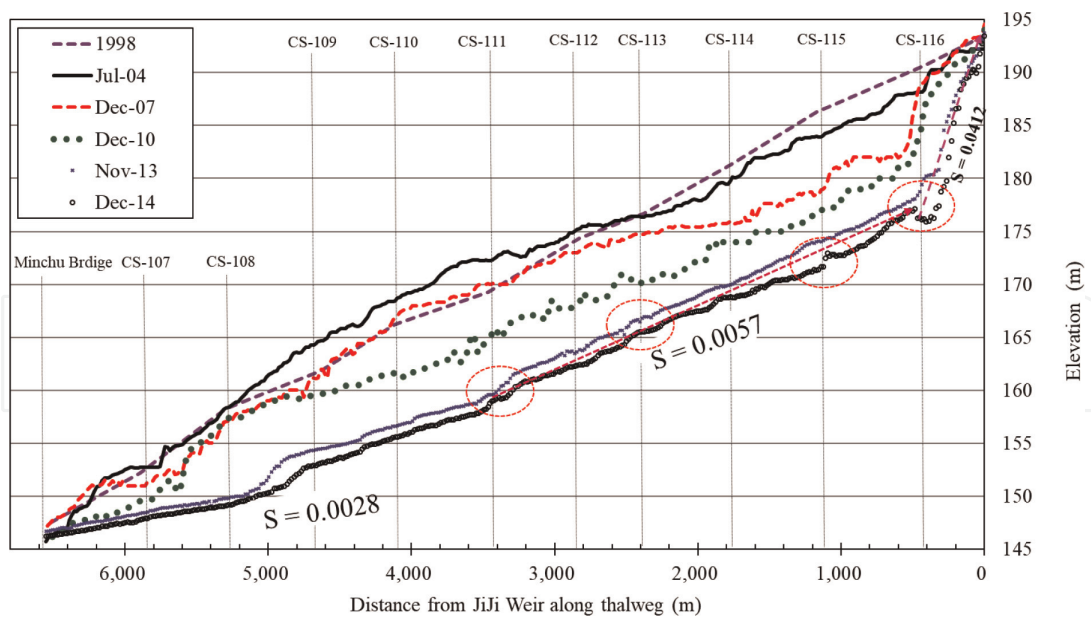


Figure 1. Historical longitudinal profiles along thalweg (S is bed slope; CS denotes “cross section”).

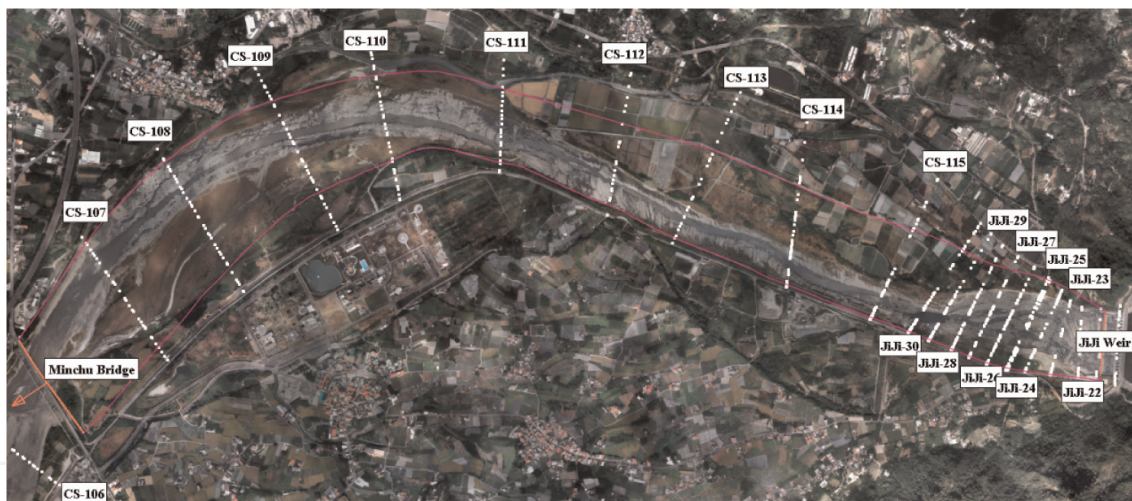


Figure 2. Study domain with survey cross sections.

about 10 m (please refer to **Figure 2** for the locations of those measured cross sections from CS-106 to CS-116). Looking downstream, **Figure 3** shows the incised channel near the JiJi Weir. The white dash line indicates the flat channel bed before the incision. The head-cut was still actively developing and migrating, which has threatened the integrity of the dam (**Figure 4**).

To prevent this channel from further erosion and protect the JiJi Weir Dam, the Water Resources Agency (WRA) of Taiwan has proposed several erosion control plans [1, 2]. Several weir structures and channel widening were proposed to promote sediment deposition and lower the water surface level for flood protection. This study is to provide alternative plans optimal for erosional control and flood protection by using a 3D numerical model, CCHE3D [3], with capabilities in simulating bedrock erosions with lateral erosions.



Figure 3.
Bedrock channel (photo by Zhang, Y., 2015.11.2; look toward downstream).

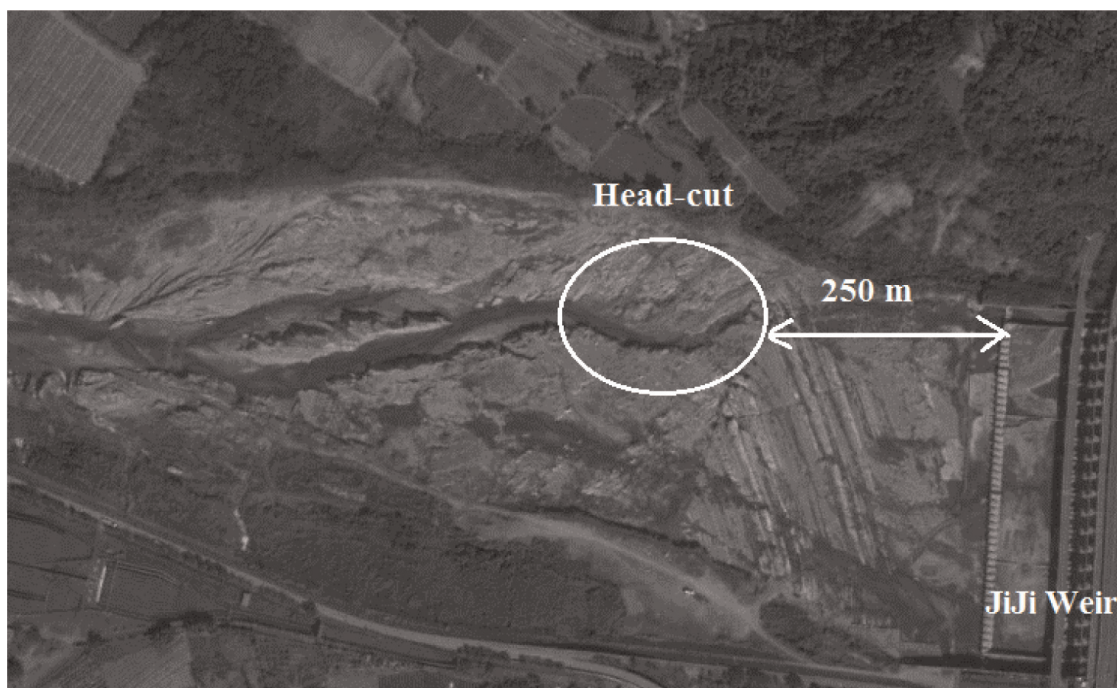


Figure 4.
Head-cut development at downstream of Jiji Weir (satellite image, 2014.11.23).

The bed rock erosion is closely related to channel lithology, tectonics, and geomorphology properties, contributed significantly by complicated weathering, plucking, abrasion (due to both bed load and suspended load), cavitation, and dissolution processes [4], which is distinguished from river sediment transport and morphologic processes on alluvial beds. Extensive research studies have been carried out

for attempting to describe these complex physical mechanisms of bedrock erosions mathematically. For examples, Annandale [5] proposed a conceptual framework to correlate the flow energy to the earth mass erodibility by introducing the erodibility index, which characterizes the capability of earth materials for resisting erosions. Whipple and Tucker [6] considered the stream power to dominate the bedrock erosions. Whipple *et al.* [4] developed the conceptual models for plucking, abrasion, and cavitation in terms of the relationship between the bed shear stress and erosion rate by studying the field erosion processes. Sklar and Dietrich [7] identified the sediment supply as an important factor for bedrock erosions due to abrasion. Sklar and Dietrich [8] proposed a mechanistic bedrock erosion model by saltating bed load based on their work in 2001. Turowski *et al.* [9] extended and improved the Sklar's approach with more detailed covering effect. Stock *et al.* [10] measured rock erosion rate in several field sites including river in the United States and Taiwan. Lamp *et al.* [11] extended Sklar and Dietrich [8]'s work further by considering the impacts from not only the bed load but also the suspended load.

From the previous studies, the fluvial impacting factors for the bedrock erosions were identified as follows: bedrock erodibility (strength), stream power, shear stress, sediment supply, and grain size. Accordingly, two types of models [12], namely the hydraulic scour model (stream power-based [5, 13]) and the abrasion scour model [8] have been used in the applications with numerical simulations. Jia *et al.* [14] incorporated the abrasion-based bedrock erosion model into CCHE2D model [15] to study the channel incisions at downstream of Jiji Weir. Lai *et al.* [12] proposed a hybrid bedrock erosion model by combining the abrasion-based model and the stream-power based model. Liao *et al.* [16] implemented a stream-power-based soft bedrock erosion model into a 2D mobile-bed model EFA (Explicit Finite Analytical) to study the channel morphological process in an uplifted reach of Ta-An River by an earthquake in Taiwan. In addition to a 2D bedrock erosion model, Jia and Zhang [1, 2, 17] first developed a 3D bedrock erosion model by extending Liao *et al.* [16]'s method to CCHE3D [3] to study the channel incision problems in Taiwan.

This chapter is to present the development and applications of the CCHE3D bedrock erosion module to study the channel incisions and erosion control problems in the downstream channel of the Jiji Weir. The numerical model was calibrated and validated using field data. Based on the evaluations of the multiple alternatives, an optimal control plan, involving multiple weir constructions with the side channel excavations as well, was proposed to control the head-cut development soft rock and the channel incision.

2. Numerical model

CCHE3D model [3] is a Finite Element Method (FEM) model based on a partially staggered 3D sigma layered mesh system, which consists of multiple layered structured meshes. It was developed for 3D numerical simulation and analysis for free surface turbulent flows in rivers, lakes, reservoirs, and estuaries and associated processes, such as sediment transport [18], morphological changes [17], heat transfer [19], pollutant transport and water quality evaluation [20], etc. Since it can provide more accurate and detailed local flow fields around in-stream structures [18] than 2D depth averaged models, CCHE3D model was selected to evaluate the erosion control plans with multiple weir structures installed in the study channel.

2.1 3D RANS model

The full 3D Reynolds-averaged Navier-Stokes (RANS) equations are solved in CCHE3D model, which are simply listed in the form of index notations for Cartesian coordinates as follows:

$$\frac{\partial u_i}{\partial x_i} = 0 \quad (1)$$

$$\frac{\partial u_i}{\partial t} + u_j \frac{\partial u_i}{\partial x_j} = -\frac{1}{\rho} \frac{\partial p}{\partial x_i} + \frac{\partial}{\partial x_j} \left(\nu \frac{\partial u_i}{\partial x_j} - \overline{u'_i u'_j} \right) + f_i \quad (2)$$

where u_i = Reynolds-averaged velocities defined at x_i ($i, j = 1, 2, 3$); t = time ; ρ is water density; p is pressure; ν is kinematic viscosity; $-\overline{u'_i u'_j}$ = Reynolds stress; and, f_i represents the body force.

For surface flows, the free surface kinematic equation is applied:

$$\frac{\partial \eta}{\partial t} + u_\eta \frac{\partial \eta}{\partial x} + v_\eta \frac{\partial \eta}{\partial y} - w_\eta = 0 \quad (3)$$

where η is water surface elevation; and (u_η, v_η, w_η) denotes velocity at water surface.

In CCHE3D model, a partially staggered stencil and a velocity correction algorithm are used for solving the momentum and continuity equation. Several turbulence closure schemes including the zero equation models (parabolic, mixing length, and wind-induced) and the $k - \epsilon$ models are provided. More details of CCHE3D model can be found in Ref. [3].

2.2 3D sediment transport model

Sediment transport is one of the most complex and least understood phenomena in nature. In 3D, sediment particles' movements are highly affected by vertical motion of fluid flows in addition to horizontal movements. This is particularly true in the vicinity of hydraulic structures where the flow impacts on the solid walls of the structures (bridge pier and abutment, for instance). If the structures are very large (dam), the fluid flows in an open channel are forced to change their speed and direction near structures in order to pass through them, the sediment transport capacity due to this impact is adjusted significantly causing localized scouring and deposition over the sediment bed. In CCHE3D model, in addition to general sediment transport capabilities, special sediment transport features, such as local scouring around structures and channel head-cut migration have been developed as well.

In CCHE3D model, the 3D convection-diffusion equation for the suspended sediment is solved as follows:

$$\frac{\partial C}{\partial t} + u \frac{\partial C}{\partial x} + v \frac{\partial C}{\partial y} + (w - \omega_s) \frac{\partial C}{\partial z} - \frac{\partial}{\partial x} \left[\frac{\nu_t}{\sigma_s} \frac{\partial C}{\partial x} \right] - \frac{\partial}{\partial y} \left[\frac{\nu_t}{\sigma_s} \frac{\partial C}{\partial y} \right] - \frac{\partial}{\partial z} \left[\frac{\nu_t}{\sigma_s} \frac{\partial C}{\partial z} \right] = ST \quad (4)$$

where C is the suspended sediment concentration; u , v , and w are velocity components (m/s); ω_s is the sediment settling velocity; ν_t is the eddy viscosity (m^2/s); ST is the source term. and σ_s is the Schmidt number to convert the turbulence eddy viscosity to eddy diffusivity for suspended sediment.

At the free surface, the vertical sediment flux is zero, so the gravity effects $\omega_s C$ balance the diffusion effects $\varepsilon_s \frac{\partial C}{\partial z}$, and the following condition is applied:

$$\omega_s C + \varepsilon_s \frac{\partial C}{\partial z} = 0 \quad (5)$$

At the bottom, the following condition is applied:

$$\omega_s C + \varepsilon_s \frac{\partial C}{\partial z} = D_b - E_b \quad (6)$$

where ω_s is settling velocity (m/s); $\varepsilon_s = \nu_t / \sigma_c$ is diffusion coefficient for sediment; D_b and E_b (kg/m²/s) are deposition rate and erosion (re-suspension) rate at bottom, respectively.

Following the non-equilibrium transport approach ($q_{bk} \neq q_{b^*k}$) proposed by Wu [21], the bedload transport rate is governed by

$$\frac{\partial(\delta \bar{c}_{bk})}{\partial t} + \frac{\partial q_{bkx}}{\partial x} + \frac{\partial q_{bky}}{\partial y} = -\frac{1}{L_b} (q_{bk} - q_{b^*k}) \quad (7)$$

where q_{bk} is the bedload transport rate for the k_{th} size class, q_{bkx} and q_{bky} are the component in x and y directions, δ is the bedload layer thickness, \bar{c}_{bk} is the bedload concentration and L_b is the bedload adaptation length; q_{b^*k} is the bedload sediment transport capacity for equilibrium transport conditions, which can be estimated using empirical transport formulas.

2.3 Bedrock erosion model

According to previous studies, the bedrock erodibility (strength), stream power, shear stress, sediment supply, and grain size were identified as important impacting factors on bedrock erosion rate, which lead to two popular bedrock erosion mechanisms, plucking and abrasion, widely used in the numerical models [1, 12, 14, 16]. The first one is corresponding to the so-called stream power-based method that the bedrock erosion rate is considered as a function of the stream power, and the varying shear stress causes the hydraulic scouring on soft bedrock [4–6, 13], and the other one is the abrasion-based method, which emphasizes on the important role of the sediment supply (both bedload and suspended load) by considering the eroding and shielding effects of sediment on bedrock [7, 8, 11].

Whipple *et al.* [4] observed in the field that for well-joined rocks with fractures and bedding planes, the plucking is the dominant erosion process, while the abrasion process dominates for rocks with smooth and polished surfaces but with ripples, flutes, and potholes prominently developed. All the aforementioned bedrock erosion models oversimplified and conceptualized the complicated bedrock erosion processes in nature. For any particular mountainous river, these natural processes cannot be separated and modeled accurately using one method. Practically, however, a certain dominant process has to be selected to represent all erosion mechanisms for the modeling purpose. For the downstream channel of Jiji Weir, since the measured bedrock erodibility is available, it is assumed that the plucking is dominating in this reach, and the stream power method [16] is selected for current study.

In the stream power method, the bedrock erosion rate E is only related to the rock erodibility index [5] and the flow stream power, which is proportional to bed shear stress, as described in Eqs. (8, 9):

$$E = K_s U \left(\frac{P}{P_{cm}} - 1 \right)^c = K_s U \left(\frac{\tau U}{P_{cm}} - 1 \right)^c \quad (8)$$

$$P_{cm} = a K_h^b \quad (9)$$

where K_s is non-dimensional coefficient; U is depth-averaged velocity of flow (m/s); P is stream power of flow (kW/m^2), $P = \tau U$, τ is shear stress (N/m^2); P_{cm} is critical stream power (kW/m^2); K_h is the bedrock erodibility index defined as the capability of earth materials for resisting erosion, which is correlated empirically to the stream power and obtained based on field and laboratory studies; and, a , b , and c are site-specific calibrated parameters.

The above stream power method is further improved to take into account lateral erosion by considering the local lateral bed slope. Thus, a factor S_b representing high slope zones is introduced as follows:

$$S_b = \max \left(\frac{S_l}{k \cdot S_R}, 1.0 \right)^r \quad (10)$$

where S_l is the local lateral bed slope computed in an element, S_R is a reference slope of the simulation area; it is currently represented by the average slope of all wet elements in a domain. The power r is empirical and needs to be calibrated. In the tests, it is found that $r = 1.5 \sim 5.0$. It can be seen that this factor is effective only when the local lateral bed slope is larger than the reference slope. $k = 1 \sim 6$ is the coefficient to adjust the reference slope, which filters out small slope area from erosion. With this factor, Eq. (8) is modified to:

$$E_{bb} = K_s U \left(\frac{P}{P_{cm}} - 1 \right)^c S_b \quad (11)$$

where E_{bb} is the erosion rate applicable to both softrock bed and bank erosion. With $r = 0$, Eq. (11) will convert back to Eq. (8).

2.4 Coupling of bedrock erosion model and sediment transport model

When the sediment transport is simulated, the boundary condition between the moving sediment particles and the bedrock has to be treated. Sediment particles can deposit over the rock surface and form a deposition layer. A concept of a sediment mixing layer over the softrock surface is adopted. If the thickness of the sediment layer is large, no rock erosion is calculated. If no sediment deposition exists on the bed, the proposed stream power method is used for the rock bed erosion. If the thickness of the sediment layer is within a criterion (mixing layer thickness), the stream-power-induced erosion would be applied at a reduced rate, proportional to the thickness of the mixing layer. The net change rate of the mixing layer is the combined rates of rock erosion and sediment deposition.

There is insufficient knowledge on the interactive and coupling mechanism between the bedrock erosion and the sediment transport. This simple coupling

basically considers the shielding effects of the sediments on bedrock, similar to that of the abrasion model, which is conceptually reasonable and has been proved and validated in previous studies [7, 8, 11]. However, the actual interactions between the bedrock erosion process and the sediment transport process are much more complicated in nature.

3. Application to downstream of Jiji Weir

In this study, CCHE3D bedrock erosion model was used to simulate the aforementioned channel incision process. The validated model was then used to evaluate erosion control plans. The study domain is a 6.5 km reach from the Jiji Weir to the downstream Minchu Bridge, where there are measured cross sections available: CS-106 to CS-116, and Jiji-30 to Jiji-22 (Figure 2).

3.1 Model setup

Based on the DEM data of 2013 and 2014, several structured meshes covering the study domain from Jiji Weir to Minchu Bridge were generated, which embed the combinations of the planned weir structures and lateral channel excavations.

As shown in Figure 5, zones representing erodible bedrocks, alluvium, structures (non-erodible), have been identified and embedded in simulation domain based on the satellite image of 2014. The erodible bedrock zone resulted from the channel incisions and head-cut development, where both the bedrock erosion and sediment transport simulations are to be conducted. The alluvial zone is covered with pebbles

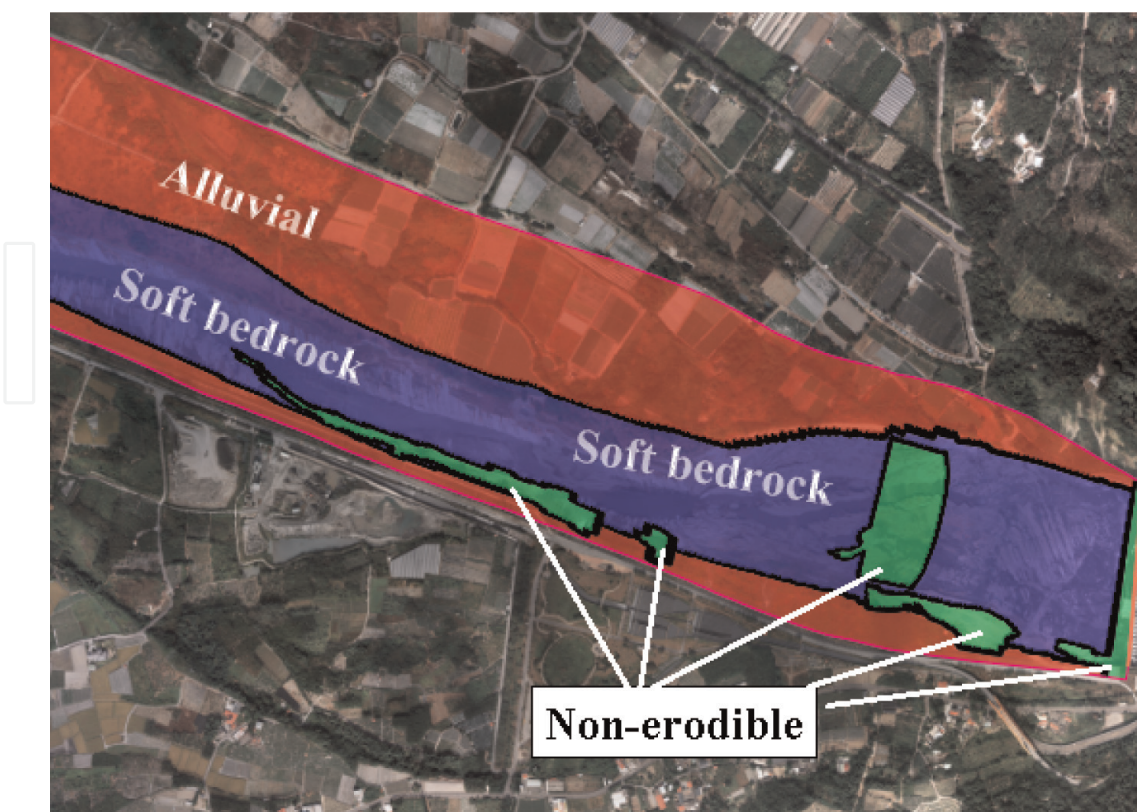


Figure 5.
Erodible bedrock zone.

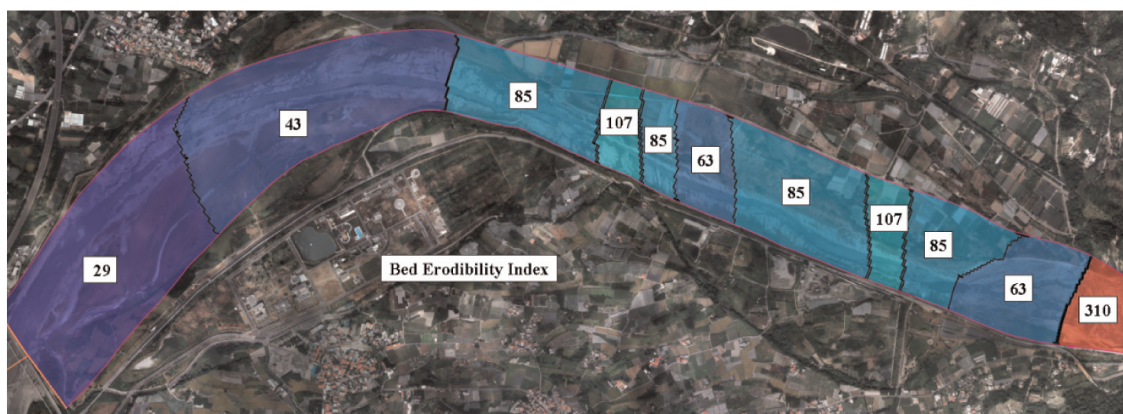


Figure 6.
 Bedrock erodibility index.

and gravels, and no bedrock erosion simulation will be applied. The non-erodible zone represents the weir structures and other bank/bed protection measures (i.e., concrete blocks) and is assumed non-erodible during the simulations. Therefore, the distribution of non-erodible zones changes with the simulated erosion control plans.

Figure 6 shows the measured bedrock erodibility index distribution in 2014. The whole domain was divided into 11 zones with different erodibility index, k_h , varying from 310 (high rock strength) to 29 (low rock strength) [2]. The aforementioned channel bed properties (**Figures 5 and 6**) are applied to all cases. Adjustments are made accordingly for the installations of weir structures in different erosion control plans.

3.2 Model calibration and validation

The site-specific parameters (a , b , and c) in Equation (8) and the lateral slope parameters r and k in Equation (11) need to be calibrated before applications. In this

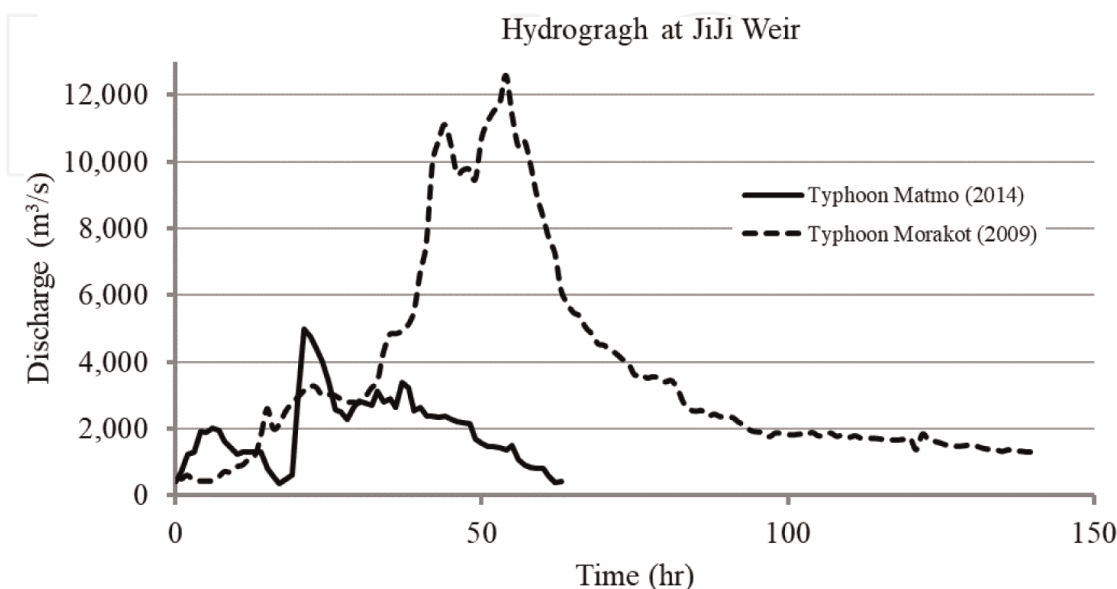


Figure 7.
 Flood hydrograph of Typhoons Morakot (8/2009) and Matmo (7/2014).

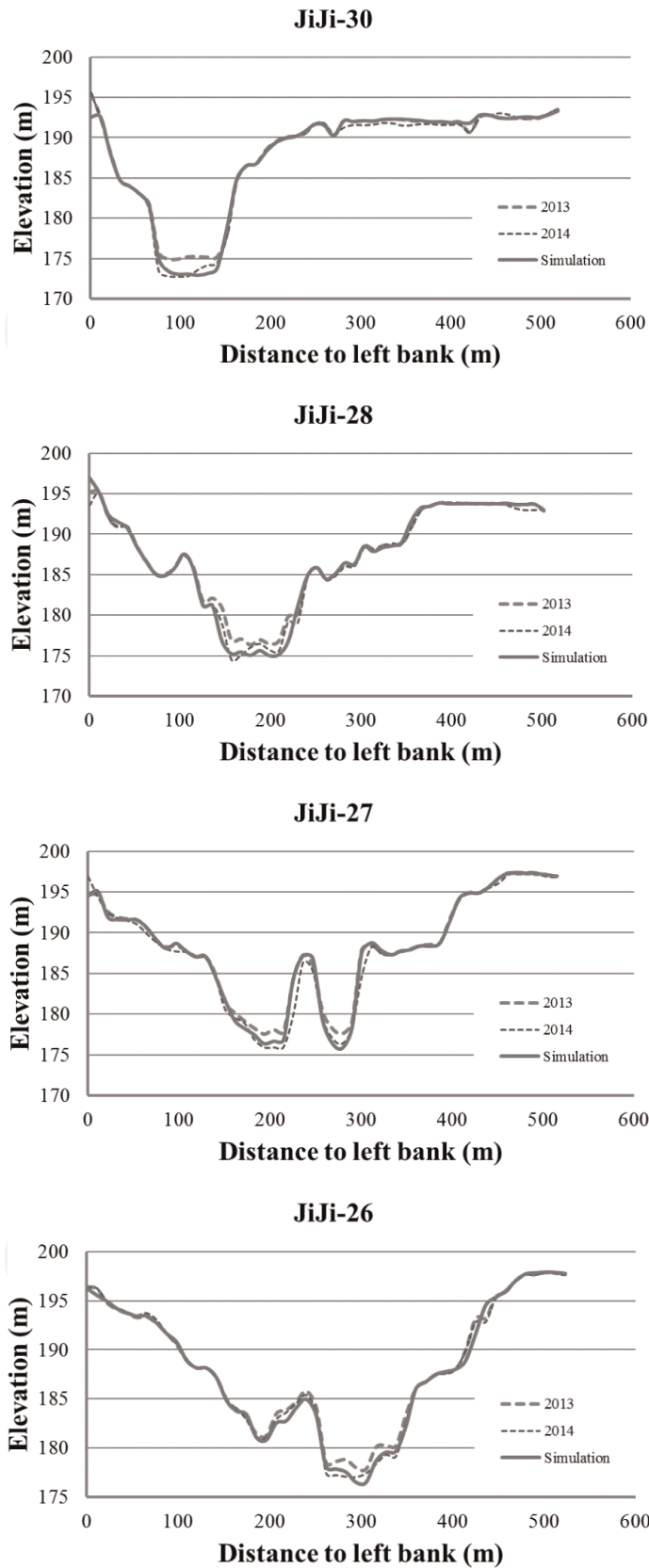


Figure 8.
Comparisons of cross-sectional profiles for Po-1 with Typhoon Matmo.

study, two cases without any control structures, P0-1 with Typhoon Marmo and P0-2 with Typhoon Morakot, are used to calibrate these parameters and validate the bed-rock erosion model, respectively.

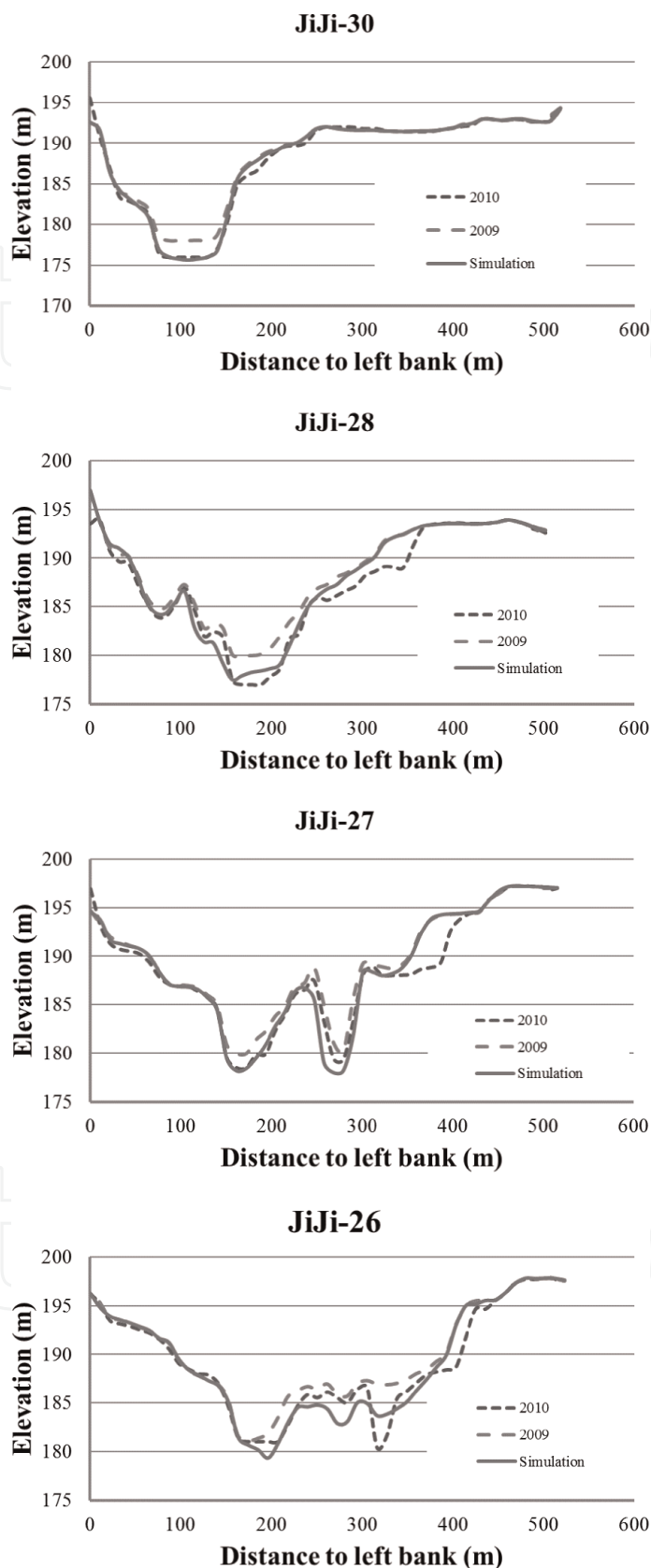


Figure 9.
Comparisons of cross-sectional profiles for Po-2 with Typhoon Morakot.

In the calibration step, the parameters are adjusted to obtain the best fit of the simulations to the data; while in the validation step, no parameters are changed. **Figure 7** shows the hydrographs of these two typhoons, which are considered as the

major hydrological events causing significant bed morphological changes in this channel. Due to its high peak discharge ($Q = 12,600 \text{ m}^3/\text{s}$), Typhoon Morakot was selected for all other erosion control plans.

Through the numerical calibration tests, the parameter set for the stream power method was found to be: $a = 0.005$, $b = 0.75$, and $c = 0.2$. For the lateral erosion effects, the slope exponential parameter $r = 1$ and the slope scale factor $k = 6$ were used. **Figures 8 and 9** compare the profiles at the selected cross sections for P0-1 with Typhoon Matmo and P0-2 with Typhoon Morakot, respectively. In general, good agreements between the measurements and the simulations were observed for both cases at those cross sections, especially for channel incisions. As for the lateral erosion observed at sections Jiji-28, 27, and 26, although more discrepancies exist, the improved stream power method with considering the slope effects (Equation 7) has proved its capability of capturing these lateral erosion phenomena in the complicated bedrock erosion processes.

3.3 Erosion control plans

Since 2007, WRA has proposed a few erosion control plans attempting to stop the downstream channel of Jiji Weir from incisions and head-cut development. These erosion control plans included multiple in-stream weir structures, lateral channel excavations, and other engineering measures, such as concrete blocks for bank protections, gabions, etc. With the calibrated and validated parameters, CCHE3D bedrock erosion model was used to evaluate all the erosion control plans with different combinations of control structures [2]. According to the numerical simulations, one plan with three weirs at Jiji-22, 25, and 26 and side excavations from Jiji-27 to CS-112 was confirmed as the most effective in the erosion reduction among all proposed erosion control plans. Based on the numerical simulations of these erosion control plans, optimal design was explored.

In the historical channel profiles along thalweg of the downstream channel from 1998 to 2014 as shown in **Figure 1**, the bed slope is 0.0412 near the head-cut reach, 0.0057 in the incision reach, and 0.0028 in the transition reach. The head-cut reach and the incision reach are of bare rock channel, actively eroded; the transition reach is sometimes partially covered with sediments, showing alluvial river morphologic and sediment transport features, and thus considered to be more stable. In this study, it is assumed that the channel will be stabilized if the bed slope can be reduced to 0.0028 approximately by installing erosion control weirs in the channel.

Since the 10 m deep head-cut has reached closer to the Jiji Dam, seriously threatening the safety of the dam structure (**Figure 3**), the protection of the upstream head-cut zone (from Jiji-30 to Jiji-22) is considered as the first priority. The high weir structure at Jiji-25 is capable of significantly reducing the bed rock erosion in the reach from Jiji-26 to Jiji-22. As for the reach from Jiji-30 to Jiji-26, a weir structure is planned at CS-115, and the small reservoir behind this weir structure is designed to slow down the flow and thus reduce the erosion.

For downstream of the head-cut zone, the deep incised main channel (from CS-109 to Jiji-26) is relatively narrow, the water surface elevation in this reach will increase during floods to endanger the embankment of the left bank. Channel lateral excavations are proposed in such a way that the thalweg is kept and the widening lateral excavation (150 m) is on the right floodplain of the channel from Jiji-27 to CS-108.5. Hydrologic data indicates that the flow discharge in the channel is less than $Q = 1000 \text{ m}^3/\text{s}$ for most time of the year, and the flows in this range are confined in the

main channel. The water depth for this discharge is about 4 m. If no in-stream weir structures are built, the proposed lateral excavations will still allow the water to flow in the deep channel for the most of time of a year, but the water will divert to the widened areas in the flood seasons. The widened channel will reduce the main flow velocity and water surface elevation, which is beneficial to bank protection during floods in addition to promote sediment deposition.

To enhance the erosion reduction effects, two additional low-headed weirs are suggested to be installed at CS-111 and CS-113 in this reach to further control the flow and erosion. To prevent the development of a second head-cut between CS-108 and CS-109 (see **Figure 1**), another low-headed weir structure is proposed as well to be installed at CS-108.5.

The heights of the four weirs at CS-108.5, CS-111, CS-113, and CS-115 are determined in such a way that the small pools formed behind the weirs can approximately protect half of the reach between weirs (slope equal to zero). As illustrated in **Figure 10**, the bed slope of the reach between Weir-A and B is S_0 , the pool behind Weir-A can affect an area about half of the reach ($L/2$). Sediments would fill up the pool behind Weir-A because the surface slope is significantly reduced. Before the deposition filled the channel segment, the bed slope behind Weir-B is larger than $S_d (= S_0/2)$, and it reaches to S_d after the segment is filled up, which is the highest slope possible in the design channel. The new established bed slope would be about half of the initial slope S_0 . The protected channel would be stable and filled with sediment. According to this idea, the top elevations of the five weirs are determined as indicated in **Table 1**.

Figure 11 shows the initial setup for the optimal design. The excavation is denoted in the white polygon area, while six weir structures installed at JiJi-25 (CS-116), JiJi-26, CS-115, CS-113, CS-111, and CS-108.5) as non-erodible zones. For the optimal design case simulations, the calibrated parameter sets and the bedrock erodibility index

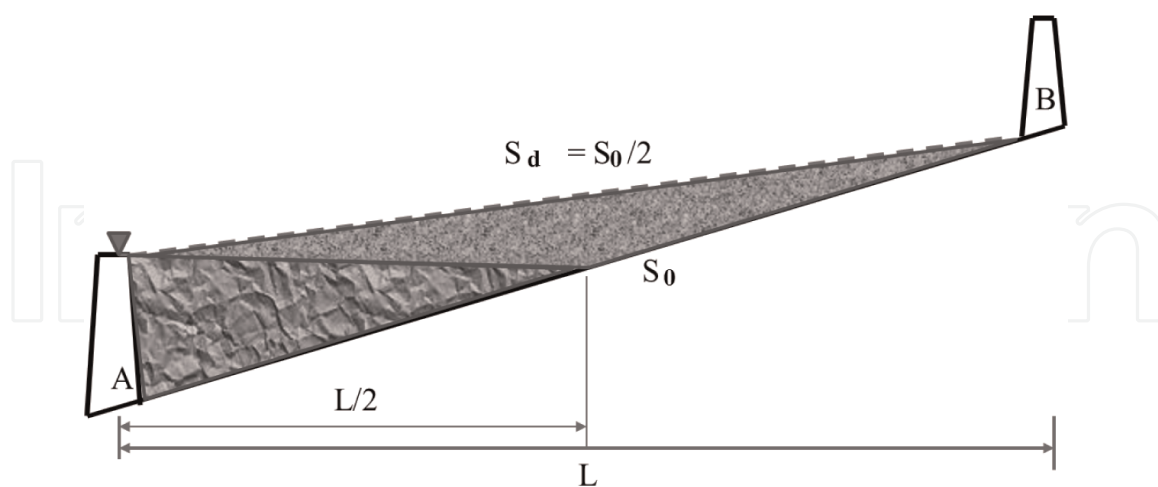


Figure 10.
 Sketch of determination of weir height.

Weirs	CS-108.5	CS-111	CS-113	CS-115	Jiji-26	Jiji-25
Elevation (m)	155.5	163	170	177	181	188

Table 1.
 Top elevations of weir structures.

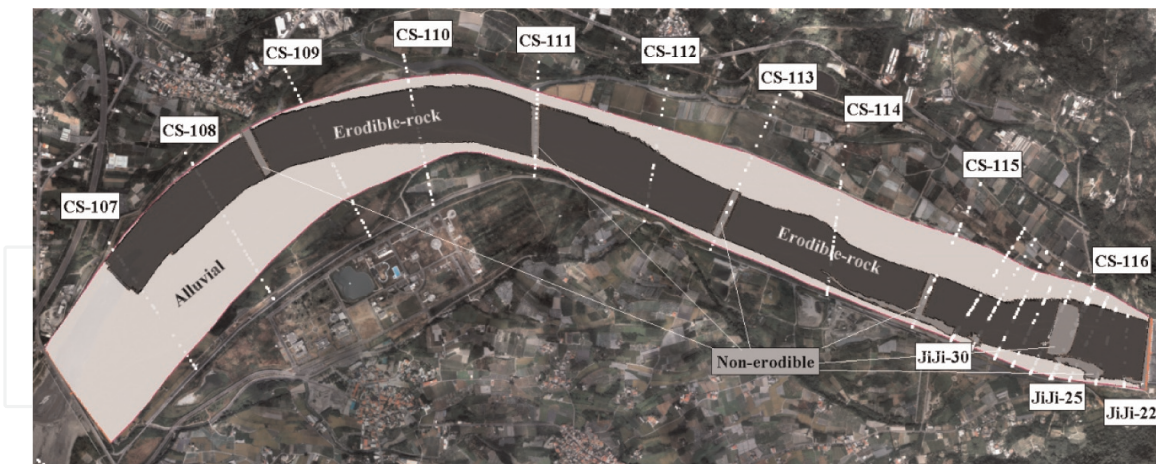


Figure 11.
Model setup for optimal design.

remain the same. The bed property zone is adjusted if the excavation cuts into the alluvium and exposes the soft rock underneath.

In current sediment transport simulations, both the suspended load and the bedload transport are considered with three representative size diameters: 0.0081, 0.03086, and 0.3006 m. Sediment boundary condition is obtained from the measured concentration in a detention pool nearby JiJi Weir during typhoon season, initial conditions and other boundary conditions are the same as the cases of stream power erosion simulations. This simply coupled sediment transport and stream-power-based erosion model was calibrated using the P0-1 conditions and then applied to sedimentation simulations in the optimal design study. The calibrated model could capture the main trend of the channel incision particularly in the reach from the JiJi Dam to CS111 under the P0-1 condition.

The simulation results of the optimal design were compared with those of the cases without any structures. **Figures 12 and 13** show the longitudinal profile of bed changes. In the first 1.2 km reach, where two high weirs at JiJi-25 and JiJi-26 are

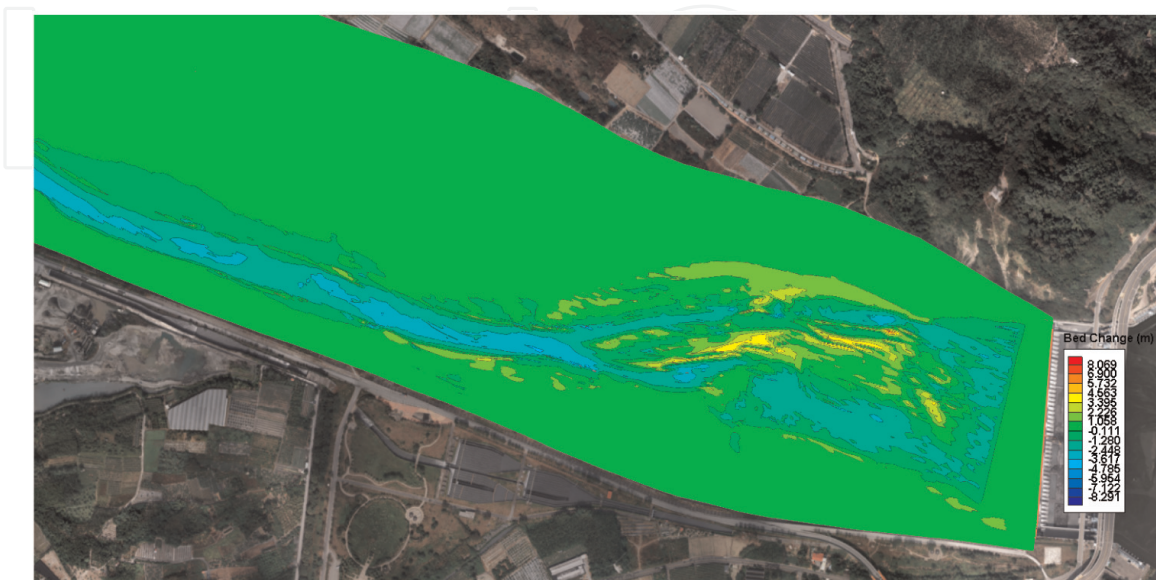


Figure 12.
Simulated erosion patterns for the case without structures.

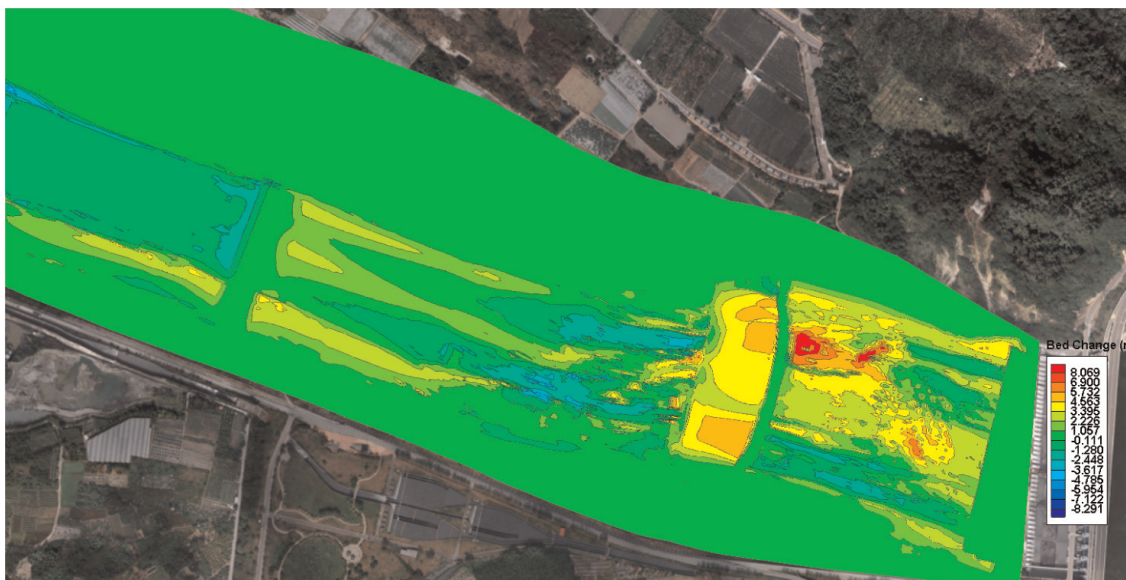


Figure 13
 Simulated erosion patterns for the case with the optimal design.

located, much more depositions were observed in the optimal plan, while the erosions are dominant for the case without structures. Further downstream, in general, the erosions are dominant for both cases, except for small regions upstream of the weir structures, where the water surface is increased, and the velocity is slower. The bed change pattern around all the weir structures is similar: there are depositions at upstream but erosions at downstream, which is expected. **Figure 14** shows the bed profile along the thalweg. As can be seen, in the optimal plan, the erosion along the thalweg has been reduced significantly, and the upstream reach with the first two weirs demonstrated obvious deposition pattern. The two weir structures at JiJi-25 and JiJi-26 do serve the purpose of reducing channel incision and stopping the head-cut development effectively (**Figure 15**).

Despite the simple coupling method, the coupled bedrock erosion and sediment transport model demonstrated the promoting effects of the proposed optimal design on sediment depositions to protect the channel bed from further eroding.

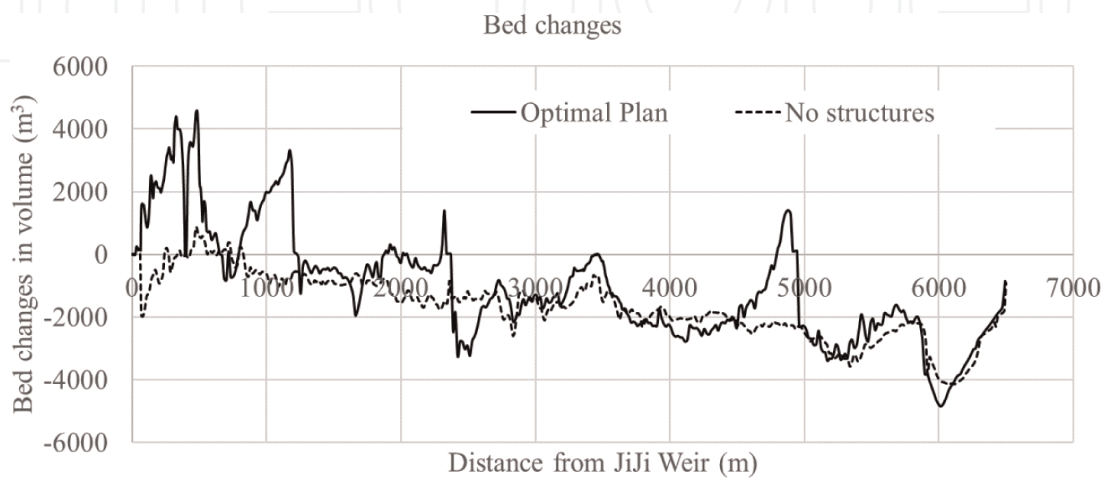


Figure 14
 Profile of bed changes.

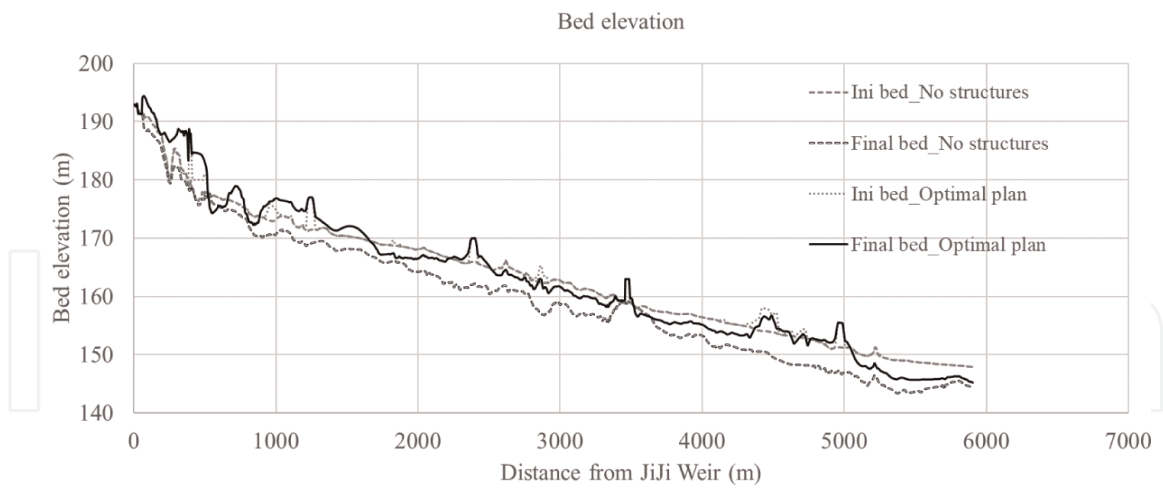


Figure 15
Profile of bed elevation along the thalweg.

3.4 Implementation of erosion control plan

The erosion control plan combined with other engineering measures (concrete blocks, gabions, and filling-ups) has been partially or completely implemented. **Figure 16** compares the aerial images of JiJi Weir in 2014 and 2021. In this 1.2 km

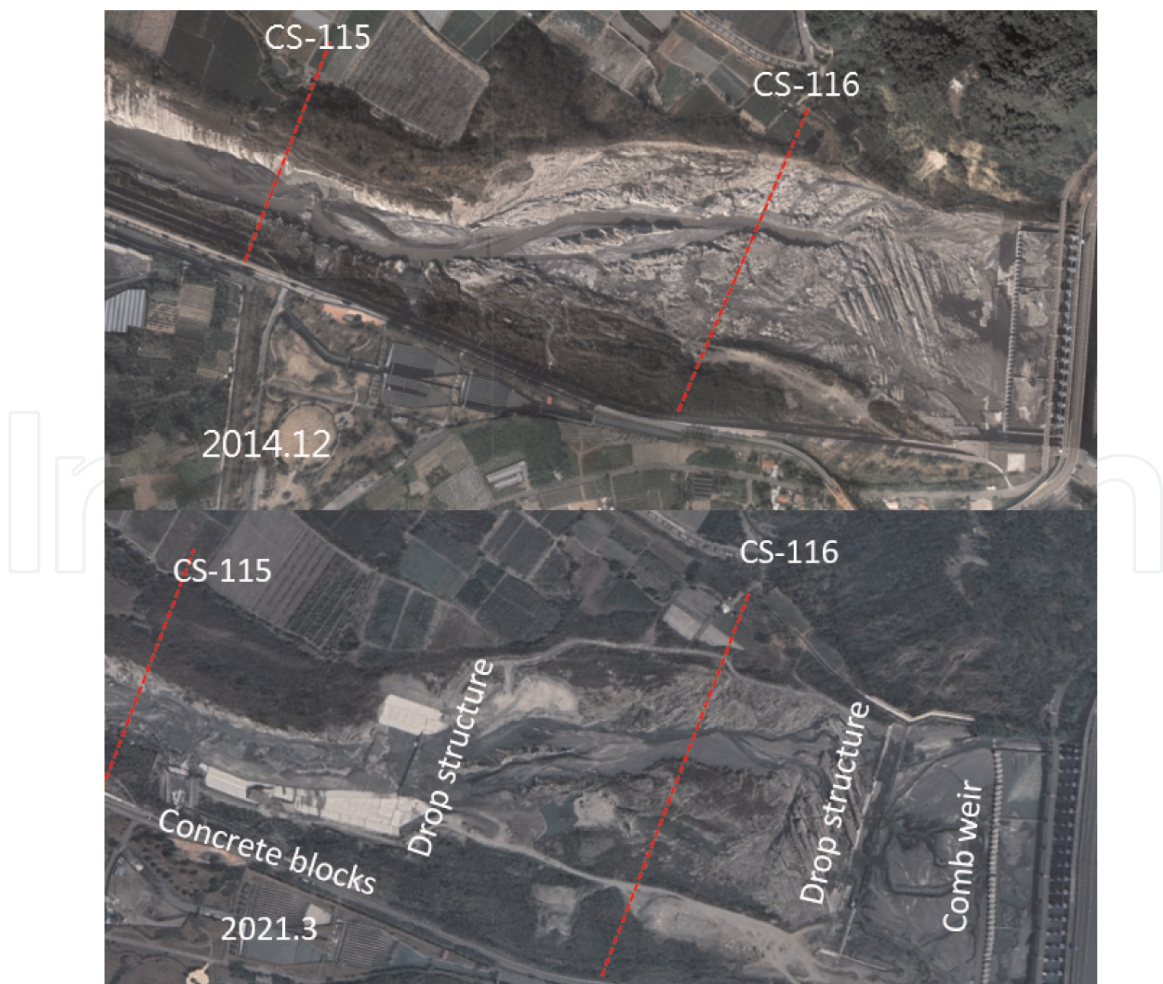


Figure 16
Aerial images of JiJi Weir.

reach of Jiji Weir downstream, a comb weir structure, two drop structures, and some concrete blocks were installed. The head-cut development from 2014 to 2021 seems not very significant, which demonstrated the effectiveness of the erosion control plan.

4. Conclusions

In this study, a simply coupled 3D bedrock erosion and sediment transport model, CCHE3D bedrock model, was developed and applied to the downstream channel of the Jiji Weir, Chushui River, where the serious channel incision and head-cut migration endanger the Jiji Dam. In this simple coupling model, a concept of a sediment mixing layer over the bedrock surface is adopted. The thickness of the sediment layer determines the bed change mechanism as follows: thick sediment layer leads to non-rock erosion calculation, while non-sediment layer indicates the dominant role of the bedrock erosion. Within the mixing layer thickness, the stream-power-induced erosion would be applied at a reduced rate, proportional to the thickness of the mixing layer. The net change rate of the mixing layer is the combined rates of rock erosion and sediment deposition.

The hydrologic data of Typhoon Matmo in 2014 and Typhoon Morakot in 2009 were used to calibrate and validate the site-specific parameters for the stream power method-based bedrock erosion model. This model was also applied to simulate the bed changes with designed channel erosion control structures installed. The objective of the study is to identify an optimal design to alleviate channel incision and stop the head-cut development.

Based on the evaluations of multiple erosion control plans proposed by WRA and the channel evolution analysis, an optimal erosion control plan was identified. Six weir structures at section Jiji-25, Jiji-26, CS-115, CS-113, CS-111, and CS-108.5 and the 150 m-wide lateral excavations from Jiji-27 to CS-108.5 along the right floodplain to widen the channel were proposed. The lateral excavation would keep flows in the thalweg, but divert the water onto the excavated area during floods. According to the longitudinal profiles along the thalweg (**Figure 1**), the CS-115, CS-113, CS-111, and CS-108.5 were selected as the locations for installing weir structures to control the channel bed slopes. The elevations of those weir structures were determined in such a way that the target weir protects a half of a segment between two neighboring weirs so that the bed slope of the pool between weirs could be reduced by half (**Figure 10**).

Using the proposed coupled bedrock erosion and sediment transport model, the optimal design and the case without any structures were evaluated and compared. According to the simulated results, the optimal design reduced the channel incision significantly, and the head-cut development was stopped by the two weir structures installed at Jiji-25 and Jiji-26. Sediment depositions were observed not only in the deep channel but also the excavated area. In general, the whole study reach from Jiji Weir to Minchu Bridge still demonstrated erosion pattern except for the first 1.2 km reach at upstream. Without any control structures, the channel would be further deepened, and the development of the head-cut would continue.

Acknowledgements

This work is a result of research sponsored by National Chiao Tung University of Taiwan under Research Agreement No. 300212267A and The University of Mississippi.

It is also a part of research sponsored by the USDA Agriculture Research Service under Specific Research Agreement No. 6060-13000-025-00D (monitored by the USDA-ARS National Sedimentation Laboratory) and The University of Mississippi.

Conflict of interest

The authors declare no conflict of interest.

Appendices and nomenclature

C	suspended sediment concentration
D_b	deposition rate (m^2s^{-1})
E_b	erosion rate (m^2s^{-1})
E_{bb}	erosion rate for both bedrock and bank erosion (m^2s^{-1})
K_h	bedrock erodibility index
L_b	bedload adaptation length (m)
q_b	bedload transport rate (m^2s^{-1})
S_b	bed slope factor
u	x velocity (ms^{-1})
v	y velocity (ms^{-1})
w	z velocity (ms^{-1})
U	depth-averaged velocity of flow (ms^{-1})
P	stream power of flow (kW m^{-2})
η	water surface (m)
ν	kinematic viscosity (m^2s^{-1})
δ	bedload layer thickness (m)
τ	shear stress (Pa)
ω^s	sediment settling velocity (ms^{-1})
σ^s	Schmidt number

Author details


Yaoxin Zhang^{1*}, Yafei Jia¹, Keh-Chia Yeh² and Chung-Ta Liao²

1 National Center for Computational Hydroscience and Engineering (NCCHE), University of Mississippi (UM), Oxford, USA

2 Natural Hazard Mitigation Research Center (NHMRC), National Chiao Tung University (NCTU), Hsin Chu, Taiwan

*Address all correspondence to: yzhang@ncche.olemiss.edu

IntechOpen

© 2022 The Author(s). Licensee IntechOpen. This chapter is distributed under the terms of the Creative Commons Attribution License (<http://creativecommons.org/licenses/by/3.0>), which permits unrestricted use, distribution, and reproduction in any medium, provided the original work is properly cited. 

References

- [1] Jia Y, Zhang Y. Preliminary Study of Local Scouring Using CCHE3D and Its Application Potential to Softrock Erosion in Choshuixi, Taiwan. National Center for Computational Hydroscience and Engineering. USA: University of Mississippi; 2013. p. 38677
- [2] Jia Y, Zhang Y. Enhancement and Application of CCHE2D/3D Soft-rock Models to Chuoshui Creek of Taiwan. National Center for Computational Hydroscience and Engineering. USA: University of Mississippi; 2015
- [3] Jia Y. CCHE3D Technical Manual, National Center for Computational Hydroscience and Engineering. USA: The University of Mississippi; 2013
- [4] Whipple KX, Hancock GS, Anderson RS. Riverincision into bedrock: Mechanics and relative efficacy of plucking, abrasion, and cavitation. *Geological Society of American Bulletin*. 2005;**112**(3):490-503
- [5] Annandale GW. Erodibility. *Journal of Hydraulic Research*. 1995;**33**(4): 471-494
- [6] Whipple KX, Tucker GE. Dynamics of the stream power river incision model: implications for height limits of mountain ranges, landscape response time scales, and research needs. *Journal of Geophysical Research*. 2005;**104**(B8): 17661-17674
- [7] Sklar LS, Dietrich WE. Sediment and rock strength controls on river incision into bed rock, *Geological Society of America. Geology*. 2009;**29**(12): 1087-1090
- [8] Sklar LS, Dietrich WE. A mechanistic model for river incision into bedrock by saltating bed load. *Water Resources Research*. 2004;**W06301**(40):1-21
- [9] Turowski JM, Hovius N, Meng-Long H, Lague D, Men-Chiang C. Distribution of erosion across bedrock channels. *Earth Surface Processes Landforms*. 2005;**33**(3):353-363
- [10] Stock JD, Montgomery DR, Dietrich WE, Sklar L. Field measurements of incision rates following bedrock exposure: Implications for process controls on the long profiles of valleys cut by rivers and debris flows. *GSA Bulletin*. 2005;**117**(11/12):174-194
- [11] Lamb MP, Dietrich WE, Sklar LS. A model for fluvial bedrock incision by impacting suspended and bed load sediment. *Journal of Geophysical Research*. 2008;**113**:F03025
- [12] Lai Y, Greimann B, Wu K. Soft Bedrock erosion modeling with a two-dimensional depth-averaged model. *Journal of Hydraulic Engineering*. 2005; **137**(8):804-814
- [13] Annandale GW. *Scour Technology, Mechanics, and Engineering Practice*. New York: McGraw Hill; 2006
- [14] Jia Y, Zhang Y, Wang S-SY. Computational Study of Softrock Erosion in a Mountain River. In: 13th Cross-Straits Symposium of Hydraulic and Water Resources. Taichung, Taiwan; 2009
- [15] Jia Y, Wang SSY. Numerical model for channel flow and morphological change studies. *Journal of Hydraulic Engineering*. 1999;**125**(9):924-933
- [16] Liao C-T, Keh-Chia K, Huang M-W. Development and application of 2-D

mobile-bed model with bedrock river evolution mechanism. *Journal of Hydro-environment Research*. 2013;8(3): 210-222

[17] Jia Y, Zhang Y. Enhancement of CCHE2D/3D Models on Softrock Erosion, Local Mesh Refinement and Their Applications to Taiwan's Rivers. National Center for Computational Hydroscience and Engineering. USA: University of Mississippi; 2014

[18] Jia Y, Scott S, Xu Y, Huang S, Wang SSY. Three-Dimensional numerical simulation and analysis of flows around a submerged weir in a channel bendway. *Journal of Hydraulic Engineering*. 2005;131(8):682-693

[19] Chao X, Jia Y, Wang SSY. 3D numerical simulation of turbulent buoyant flow and heat transport in a curved open channel. *Journal of Hydraulic Engineering*. 2009;135(7): 554-563

[20] Chao X, Jia Y, Shields FD Jr, Wang SSY, Charles M. Three-dimensional numerical modeling of water quality and sediment-associated processes with application to a Mississippi Delta Lake. *Journal of Environmental Management*. 2009; 91(7):1456-1466

[21] Wu W. CCHE2D Sediment Transport Model, Technical Report No. NCCHE-TR-2001-3, NCCHE, The University of Mississippi